Analytical Studies on Shrinkage Stress Distribution in GMA and pulse current GMA welds of thick wall stainless steel pipe having narrow and V-groove design

P.K. Ghosh[1*], Ravi Ranjan Kumar[1] and K. Devakumaran[1]
1. Dept. of Met. & Mat. Engg. , Indian Institute of Technology- Roorkee
* Corresponding Author

ABSTRACT

Analytical studies on mode, magnitude and distribution of shrinkage stress in eight quadrants of a thick wall stainless steel pipe weld have been carried out. The studies have been conducted on GMA and pulse current GMA welds prepared by using conventional-V and narrow weld groove designs at different welding parameters. The effects of all such variables on the said aspects of transverse shrinkage stress have been analysed. During welding, different quadrants of pipe are found to experience shrinkage stresses of non uniform mode and magnitude and they further varies as a function of welding process, procedure and parameter. Use of P-GMAW comparatively lowers and results better uniformity in transverse shrinkage stress distribution at different quadrants of the pipe weld than that observed in case of using GMAW. Keeping higher heat input and the pulse parameter giving larger value of their summarised influence defined a well known factor () results higher shrinkage stress. The dimensionless factor is defined as. $\phi = [(I_b / I_p) f . t_b]$. At a given heat input the narrow groove weld joint gives comparatively less transverse shrinkage stress. X-ray radiography of defect analysis reveals that the quadrants having compressive mode of stress gives rise to more lack of fusion at groove wall.

Key Words: 304LN Stainless steel pipe, P-GMAW, Pulse parameters, Narrow gap weld, Shrinkage stress, X-ray radiography

INTRODUCTION

Joining of thick wall piping systems, used in chemical, fertilizers as well as thermal and nuclear power industries are often carried out by shielded metal arc welding (SMAW) process along with gas tungsten arc welding (GTAW) root pass [1-4]. However, due to its several merits of producing comparatively cleaner and continuous weld deposition with automation, the use of gas metal arc welding (GMAW) is becoming widely popular in all these applications especially when the safety and reliability of weld joint become of prime importance. During multi-pass weld deposition in thick section the weld metal undergoes localised solidification shrinkage [4-6] followed by repetitive influence of thermal cycles from subsequent weld passes affecting the stresses developed in weld groove up to certain extent and finally causes a continuous change in groove size [6, 7] with every weld passes. It is also noticed [5, 7] that such change in groove size, affecting the groove angle, at all the locations of different quadrants of pipe weld is not uniform. The change in groove size becomes fairly large in reference to weld location and welding passes, which appreciably changes the angle of approach (attack) between the groove wall and electrode due to fixed positioning of GMA welding torch. A significant reduction in angle of attack below a minimum requirement [7, 8] may cause lack of groove wall fusion [7-10] due to lowering of energy density on groove surface at a given energy input resulting from an increase of its area of contact with the arc and thus impairs the quality of weld joint. In corroboration to this fact such lack of fusion in groove wall has been marked of varied extent at different locations of weld joint during welding of thick wall stainless steel pipe [4, 7]. However, it is noticed that the change in groove size due to shrinkage is comparatively more in case of V-groove welding as compared to that observed in case of narrow groove welding [4, 7]. This is because the latter one has relatively less weld metal deposition in comparison to that of the former one.

In case of manual welding of thick wall pipe by shielded metal arc welding (SMAW) process, the welder can somehow manipulate the angle of attack during welding to maintain an acceptable weld quality having required groove wall fusion which is not possible for continuous semiautomatic welding process like GMAW. It requires an automatic programmed system for manipulation of torch positioning during welding based on the knowledge of shrinkage stresses developed at different locations of pipe welding. A system that can automatically adjust the positioning of electrode or welding torch to maintain a minimum angle of attack to groove wall all along the circumferential path of weld deposition may solve this problem. However, it requires an analytical judgement on the basis of knowledge on characteristic shrinkage and distortion of the pipe weld at every segment of its circumference, which necessitates a clear under-standing of the nature of distortion as a function of weld deposition through each weld pass. It may be assumed that the distortion in weld groove primarily arises due to development of transverse shrinkage stress (σ_{tr}) from nature of solidification of weld deposit depending upon plate thickness as well as heat content and cooling rate of the weld pool comprising the amount of weld deposit and the fused base metal [11]. Thus, an estimation of σ_{tr} in each quadrant of a pipe weld may lead to development of suitable empirical correlation and algorithm for semi-automation of GMA welding of thick pipe. It may be more useful for the automation of narrow groove GMA welding of thick wall pipe, especially by using pulse current where, the torch manipulation becomes far more critical due to presence of highly stringent tolerance than it is there in a wider V-groove.

In this investigation an effort has been made to analyse the magnitude and mode of transverse shrinkage stresses (σ_{tr}) developed in various quadrant of a thick wall stainless steel pipe weld during continuous weld deposition in each lap using GMA and pulse current GMA (P-GMA) welding processes with different procedures. The procedural aspects of welding have been relevantly varied with a change in weld groove design from relatively wider V-groove to narrow groove. The comparative observations of this work may provide knowledge to handle appropriate manipulation of electrode approaching the groove wall during semiautomatic/automatic narrow gap GMA and P-GMA welding of thick wall stainless steel pipe.

PIPE WELDING AND MEASUREMENT OF SHRINKAGE

In this investigation the analytical studies have been carried out in consideration of the reported [4, 7, 12] characteristics of GMA and P-GMA welded butt joints of grade AISI 304LN stainless steel pipe having wall thickness and inner diameter of 25 and 300mm respectively. The semiautomatic welding of pipe was performed on 1-GR position by clamping its one end in a three jaw chuck leaving other end free for circular rotation around the same axis, where the welding torch was fixed in a rigid fixture as shown in Fig. 1. The weld joints were prepared using different procedures and parameters employed by laying eight layers of 308L stainless steel weld deposit in clock wise direction to fill the weld groove. The inter-pass welding temperature was kept as 50°C. Based on their feasibility to produce sound weld, the butt welding of pipe using GMAW was carried out by using conventional V-groove as schematically shown in Fig. 2(a). Whereas, P-GMA welding of the pipe was carried out by using both the conventional V-groove and narrow weld groove having initial groove opening of 13 mm (NG-13) as shown in Fig. 2(b). During welding the angle of attack of the torch to groove wall was consequently varied at different locations of weld in each pass of welding due to complex radial bending deformation in weld zone resulting from varied transverse shrinkage in different locations of pipe weld. The possibilities of variation in groove size by movement of groove wall in inner and outer directions, which may arise during welding due to direct and indirect effect of shrinkage of weld metal at different locations of pipe weld, are schematically presented in Figs. 3 (a) and (b). The change of angle of approach between the filler electrode to groove wall from the initial setting of ? to ?' resulting from the variation in groove size is also schematically shown in Fig. 3. The concept of change in angle of approach as it may happen due to shifting of groove wall during weld deposition even in a narrow weld groove has been conceived as schematically shown in Fig. 4.

The transverse shrinkage per weld pass has been measured by using Vernier calliper having least count of 0.01 mm. It was measured at a given initial straining length of 80 mm at 8 different quadrant location of the pipe. After each weld pass the transverse shrinkage was measured [7] at some locations of eight different quadrants along the entire circumference of the pipe weld as schematically shown in Fig. 5. The values of transverse shrinkage obtained [4, 7, 12] during welding under different welding process, procedure and parameter have been given in Table-1. Considering the Eq.2 the transverse shrinkage stress was estimated and in order to validate the measurement, it is compared with the measured residual stresses under various welding process and procedure and parameters as reported earlier [4, 7, 12] and also reproduced in Table-1. The variation in magnitude, nature and distribution of transverse shrinkage stresses at the weld has been primarily compared and studied with respect to the welding process, weld groove design and heat input. However, in case of the P-GMA weld, besides the influence of heat input the effect of pulse parameters on transverse shrinkage stresses of the weld has also been studied by considering their summarised influence estimated by an earlier reported [13-15] dimensionless hypothetical factor defined as follows.

$$\phi = [(I_b / I_p) f . t_b] \quad (1)$$

Where, (I_p) is the pulse (peak) current, (I_b) is the base current, (t_b) is the pulse off time and (f) is the pulse frequency.

ESTIMATION OF TRANSVERSE SHRINKAGE STRESS

The estimation of transverse shrinkage stress ($\sigma_{tr(i-j)}$) of a given location of pipe weld is generally considered [16, 17] as a function of heat input and plate thickness. The transverse shrinkage stresses develop during solidification of weld deposit are primarily governed by the heat content and cooling rate of weld pool comprising the amount of weld deposit and the fused base metal [11, 18]. The transverse shrinkage stresses developed in various quadrant of thick wall pipe weld has been analysed on the basis of measured variation in groove opening resulting from shrinkage during welding under different welding processes, procedures and parameters [4, 7, 12]. For an appropriate assessment of transverse shrinkage stress under varied thermal behaviour it is estimated through evaluation of measured transverse shrinkage ($\Delta_{tr(msd)}$), number of passes and average thickness of weld metal deposited per layer as follows.

$$(\sigma_{tr(i-j)}) = \frac{(\Delta_{tr(msd)})}{N} \times \frac{a}{h} \times \frac{E}{L_s} \quad (2)$$

Where,

$\Delta_{tr(msd)}$ = Transverse shrinkage (mm)
N = Number of weld layer
E = Modulus of elasticity (GPa) = 200 GPa
Ls = Straining length (Fig. 5) = 80 mm
h = Wall thickness of pipe = 25 mm
a = average thickness of weld metal deposited per layer = h/N mm.

After calculating the transverse shrinkage stress ($\sigma_{tr(i-j)}$)at each location of the pipe weld, the average transverse shrinkage stress (σ_{avg}) generated in entire pipe weld divided in eight quadrants along with its standard deviation has been estimated as follows.

$$(\sigma_{avg}) = \sum_{i=0}^{8} \frac{\sigma_{tr(i-j)}}{8} \quad (3)$$

Standard deviation =

$$\sqrt{\frac{1}{8} \times \sum_{i=0}^{8} (\sigma_{(i-j)} - \sigma_{avg})^2} \quad (4)$$

Based on estimation of transverse shrinkage stress at different locations of pipe weld, the transverse shrinkage stress ($\sigma_{tr(i-j)}$) at its each quadrant (Fig. 5) has been estimated by considering the average of transverse shrinkage stress ($\sigma_{tr(i-j)}$) at the end points of any quadrant denoted by starting and ending as (i) and (j) respectively (Fig. 5) as follow.

$$\sigma_{tr(i-j)} = \frac{(\sigma_{(i-j)}) - \sigma_{(i-j)}}{N}$$

RESULTS AND DISCUSSIONS

The transverse shrinkage measured ($\Delta_{tr(msd)}$) at 8 different locations of pipe during welding using various processes, weld groove size and parameters has been reported elsewhere [4, 7, 12] as also given in Table-1. In consideration of ($\Delta_{tr(msd)}$), the process of estimation of $\sigma_{tr(i-j)}$, σ_{avg} and $\sigma_{(i-j)}$ has been typically shown in Table-2 for V-groove weld joint prepared by GMAW process at a given heat input of 10.7 kJ/cm. The estimated transverse shrinkage stresses under different welding processes, procedure and parameters are listed in Table-3. The estimated magnitude of transverse shrinkage stresses are broadly of similar order as reported by other workers [19, 20]. The table shows that there is wide variation in transverse shrinkage stresses in different locations of weld joints and it also significantly varies with respect to welding process, procedure and groove design. By considering the average transverse shrinkage stress is lying on circumference the positive and negative deviations from it referred as tensile and compressive mode of stresses in excess respectively at different quadrants of the pipe are demonstrated on a circle.

Transverse Shrinkage Stress in V- Groove GMA Weld

The variation of nature and magnitude of transverse shrinkage stresses at different locations of GMA welded pipe has been shown in Fig. 6. The pipe was welded using V-groove and heat input of 10.7 kJ/cm. The figure reveals that the transverse shrinkage stresses present in the quadrants of 1-2, 4-5, 5-6, 6-7 are of tensile and in quadrants of 2-3, 3-4, 7-8 and 8-1 are of compressive mode. The average transverse shrinkage stress in weld is estimated as 247 ± 11.2 MPa, which is relatively less but in close approximation to the reported measured residual stress of 275 MPa [7, 12]. The difference may be considered practically insignificant in view of generally understood heterogeneity of any arc welding process.

Transverse Shrinkage Stress in V- Groove P-GMA Weld

The effect of different combinations of heat input and ϕ on variation of transverse shrinkage stress at different locations of V-groove P-GMA welded pipe has been shown in Figs. 7, 8, 9 and 10. It is observed that at low heat input of the order of 7.7-8.0 kJ/cm the change in pulse parameters causing an increase of the factor ϕ from 0.05 to 0.25 relatively enhances the magnitude of average transverse shrinkage stress from 207 to 213 MPa. It also enhances the variation in magnitude of stress distribution along different quadrant of the pipe weld. However, at higher input of the order of 9.1-9.4 kJ/cm the average transverse shrinkage stress is found relatively higher than that of the low heat input weld and it further increases also with the increase of ϕ from 0.06 to 0.25. A maximum estimated average transverse shrinkage stress of about 236 MPa is found at the heat input of 9.4kJ/cm having ϕ of 0.25.

Transverse Shrinkage Stress in Narrow Groove P-GMA Weld

The effect of different combinations of heat input and pulse parameters of varying ϕ on change of transverse shrinkage stress at different locations of narrow groove P-GMA welded pipe has been shown in Figs. 11,12 and 13. It has been observed that an increase of heat input from about 7.4 to 9.2 kJ/cm increases the magnitude of estimated average transverse shrinkage stress to a maximum of 195 ± 11.6 MPa. However, it is interestingly observed that at low heat input with low value of ϕ the transverse shrinkage stress is estimated of the order of 166 MPa, which is appreciably lower than the estimated average transverse shrinkage stress of the weld prepared by using other welding processes and procedures. In this case the stresses in the initial four quadrants have been found of compressive mode while in the last four quadrants they are of tensile mode (Fig. 11). The above observations infer that the use of narrow groove P-GMA welding process considerably reduces the average transverse shrinkage stress of thick wall pipe weld in comparison to that develops in other welds prepared by conventional GMAW processes. Keeping a low heat input and low ϕ in P-GMAW favours a further reduction of shrinkage stress in weld joint.

Stress Distribution Affecting Quality of Pipe Weld

In consideration of the X-ray radiographs of these pipe welds as reported earlier [7], the effect of stress distribution at its different quadrant on weld quality with respect to lack of fusion in groove wall has been analysed. The X-ray radiography results of pipe weld has been shown in Table-4. Correlation of the mode, magnitude and distribution of transverse shrinkage stresses (Figs. 6-13) with the X-ray radiography analysis of lack of fusion at different locations of the pipe welds (Table-4) shows that the lack of fusion at groove wall largely occurs in the quadrants of the having compressive stresses. This may have primarily happened because with the development of compressive stresses the groove becomes comparatively narrower (Fig. 3(a)) and thus reduces the angle of attack of arc in reference to the fixed position of welding torch. It causes larger surface area of heating at the groove wall and minimizes energy density on groove wall resulting in a lack of fusion to it.

CONCLUSIONS

The observations on mode, magnitude and distribution of transverse shrinkage stress at different quadrants of thick wall stainless steel pipe weld prepared by using GMA and P-GMA welding processes with varied weld groove size and welding parameters may be concluded as follows.

1. The mode and magnitude of transverse shrinkage stresses develop in each quadrants of thick wall pipe weld is different from each other.
2. The use of P-GMAW process results comparatively low and more uniform transverse shrinkage stress distribution at different quadrants of the pipe weld than that observed in case of using GMAW process.
3. At a given heat input a change in pulse parameter giving larger value of (ϕ) results higher shrinkage stress but at a similar order of an increase in heat input increases the shrinkage stress more significantly.
4. At a given heat input the narrow groove weld joint gives less transverse shrinkage stress as compared to conventional V-groove weld joint.
5. The defect analysis of weld by X-ray radiography reveals that the lack of fusion at groove wall primarily exists in the quadrants having compressive mode of stress in pipe weld.

The study throws some light on the basic understanding of thick wall pipe welding with respect to development of stresses in it. It may also help in appropriate control welding procedure as well as to introduce automation in narrow gap GMAW and P-GMAW process for welding of thick wall pipe.

REFERENCES

1. Baldev Raj, Mudali, K., Vasudevan, M. and Shankar, P, [2002], "Current status on AISI types 304 LN and 316 LN austenitic stainless steels", Special Issue on High Nitrogen Steels Part A, Trans. Ind. Inst. for Metals, Vol.55 (4), pp.131-147.

2. Clark, J. and Goswami, T., [2002], "Life prediction of stainless steels used in nuclear reactors", Mechanical Behavior of Materials, Vol. 13(5-6), p 273-282.

3. Han, H.Y. and Sun, Z., [1999], "Development of Welding Wire for High-Purity Austenitic Stainless Steels", Welding Journal, Vol.78 (2), pp. 38s-44s.

4. Ghosh, P.K., Kulkarni, Shrirang., Singh, P.K. and Vaze, K.K., [2007], "Superiority of Narrow Gap SMA Welding of 304LN Stainless Steel Pipe", Indian welding Journal, October, pp. 44-57

5. Deng, D., Murakawa, H. and Liang, W., [2008], "Numerical and experimental investigations on welding residual stress in multi-pass butt-welded austenitic stainless steel pipe", Computational Materials Science, Vol. 42, pp. 234-244.

6. Dong, P., [2001], "Residual stress analyses of a multi-pass girth weld: 3-D special shell versus axisymmetric models", Journal of Pressure Vessel Technology, Vol.123, pp.207-213.

7. Kulkarni, Shrirang, [2008], "Narrow Gap Pulse Current GMAW of Thick 304LN Stainless Steel Pipe", PhD Thesis, Metallurgical & Materials Engineering Department, IIT Roorkee.

8. Innyi, T., [1975], "Narrow gap welding for corner joint in box grinder made of heavy high tensile strength (80 Kg/mm class) steel", Advanced Welding Technology, Japan Welding Society, pp. 387-390.

9. Fricke, S., Keim, E. and Schmidt, J., [2001], "Numerical weld modelling - a method for calculating weld-induced residual stresses", Nuclear Engineering and Design, Vol. 206, pp.139-150.

10. Futamura, K., [1978], "Application of narrow gap automatic welding process to heavy steel structures of building", Australian Welding Journal, pp.37-40

11. Radaj, D., [1992], "Heat Effecting of Welding", New York, Springer-Veralag, pp.182-200.

12. Kulkarni, S.G., Ghosh, P.K., and Ray, S. [2008], "Improvement of weld characteristics by variation in welding processes and parameters in joining of thick wall 304LN stainless steel pipe", ISIJ Int., Vol.48, pp.1560-1569.

13. Ghosh, P.K., Gupta, S.R., and Randhawa, H.S., [1999], "Characteristics and criticality of bead on plate deposition in pulsed current vertical-up GMAW of steel", International Journal for Joining of Materials, Vol. 11, No. 4, pp. 99-110.

14. Ghosh, P.K., Gupta, S.R. and Randhawa, H.S., [2000], "Characteristics of a pulsed-current, vertical up gas metal arc weld in steel", Metallurgical Transactions A, Vol. 31A, pp.2247-2259. 15. Ghosh, P.K., Dorn, L., Devakumaran, K., Hofmann, F., [2009], "Pulsed current gas metal arc welding under different shielding and pulse parameters; part-1: Arc Characteristics" ISIJ Int., Vol. 49(2), pp. 251-260.

16. Kou, Sindo, [2003], "Welding Metallurgy", edition 2, A John Wiley & sons, Interscience, Publication, pp. 122-130.

17. Panin, V.N. [2007], "Experimental-Calculation Estimation of Residual Welding Distortion in Shells of Turbine Penstocks at Hydraulic Power Stations", The Paton Welding Journal, pp. 7-11.

18. ASM Handbook, [1993], "Welding, Brazing, and Soldering", vol. 6, ASM International, Materials Park, Ohio, pp. 559-618. 19.Ghosh, P.K., Devakumaran, K., Pramanick, A.K., [2008], "Effect of Pulse Current on Shrinkage Stress and Distortion in Multi-Pass GMA Weld Of Different Groove Size", Welding Journal, Under Review.

20. Chakrapani Basavaraju [2000], "Simplified analysis of shrinkage in pipe to pipe butt welds", Nuclear Engineering and Design, Vol. 197, pp.239-247.

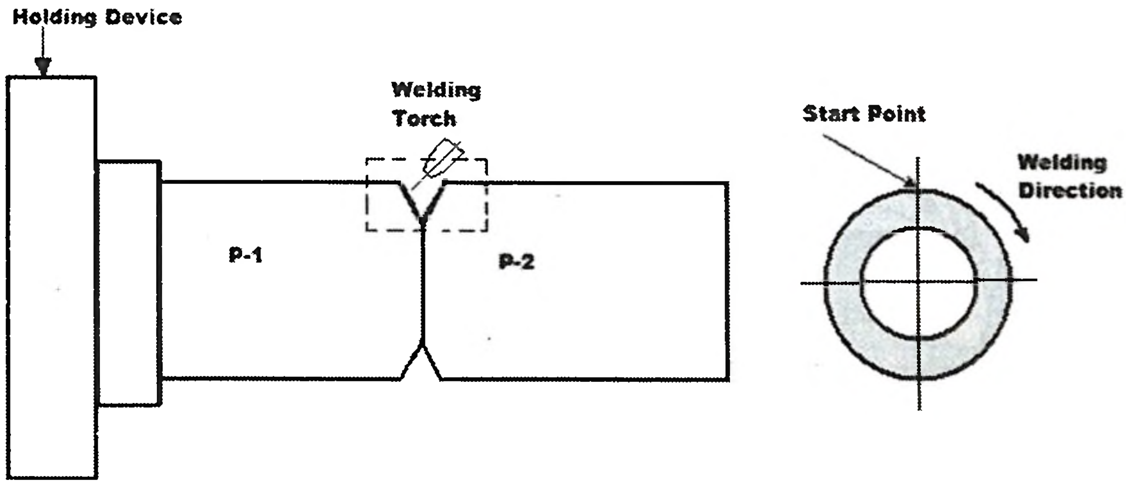

Fig.1 : Schematic diagram showing welding arrangement for pipe weld

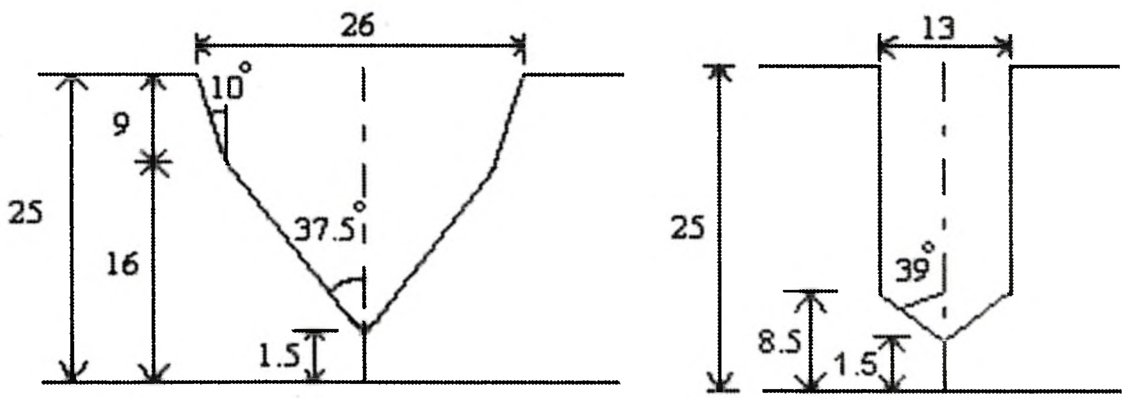

Fig.2 : Schematic diagrams of
(a) V-groove and (b) narrow groove of 13 mm groove width (NG-13)

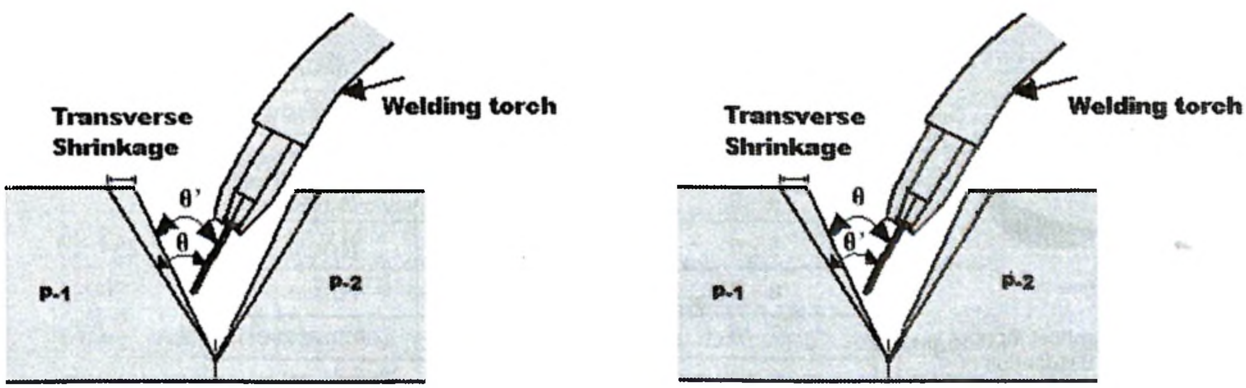

Fig.3 : Schematic diagram showing the change in angle between the electrode
to groove wall due to wall movement during welding process causing
(a) reduction in groove width and (b) increase in groove width

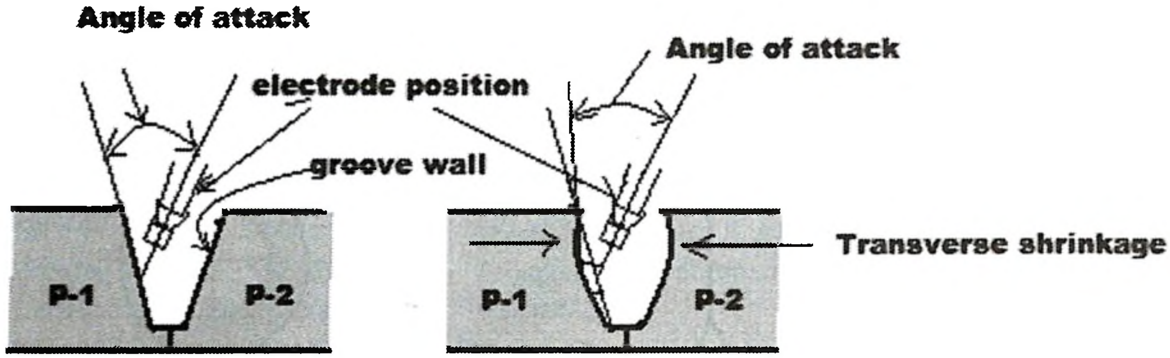

Fig. 4 : Schematically conceived view of change in angle between the electrode to groove wall during narrow-groove welding

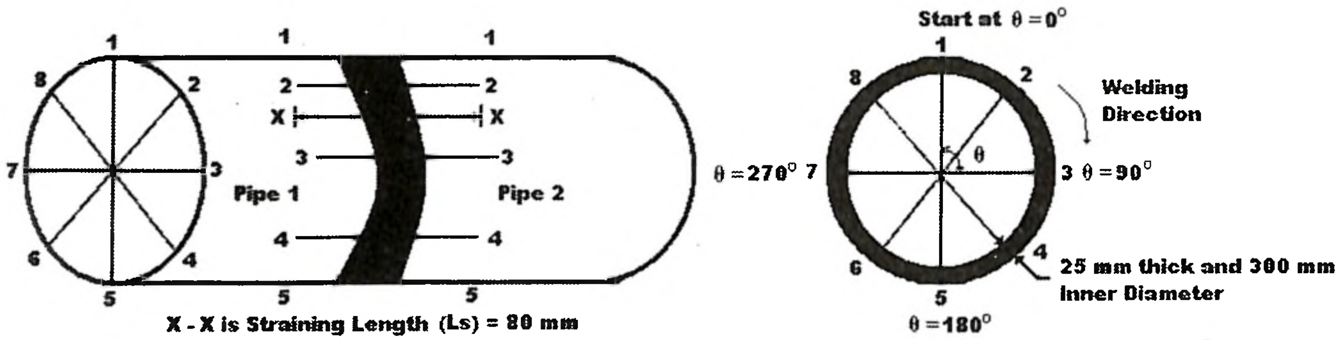

Fig. 5 : Schematic diagram of measurement of transverse shrinkage at different locations of pipe weld

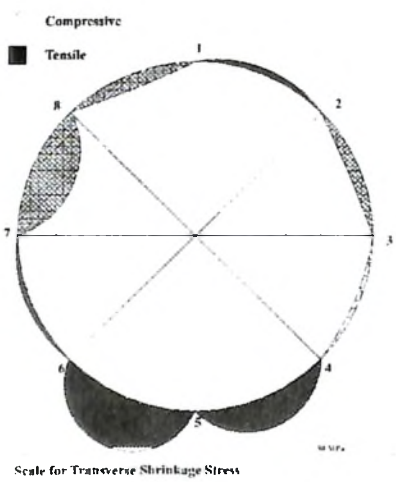

Fig. 6 : At a given heat input of 10.7 kJ/cm the distribution of transverse shrinkage stress at diferent quadrants of pipe weld prepared by using GMAW and conventional V-Groove

Weld location	Transverse Shrinkage Stress (MPa)	Nature	Avg. Transverse Shrinkage Stress ± Std.Dev.
1 - 2	256.64	Tensile	
2 - 3	249.25	Compressive	
3 - 4	251.80	Compressive	
4 - 5	267.60	Tensile	
5 - 6	276.70	Tensile	254 ± 1.1
6 - 7	255.61	Tensile	
7 - 8	234.86	Compressive	
8 - 1	247.51	Compressive	

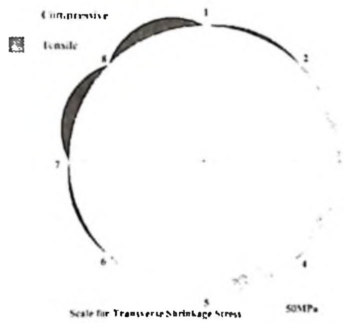

Fig. 7 : At a given heat input and ϕ of 7.7 kJ/cm and 0.05 respectively the distribution of transverse shrinkage stress at different quadrants of pipe weld preparedby using P-GMAW and conventional V-Groove.

Weld location	Transverse Shrinkage Stress (MPa)	Nature	Avg. Transverse Shrinkage Stress ± Std.Dev.
1 - 2	208.6	Tensile	
2 - 3	204.7	Compressive	
3 - 4	202.0	Compressive	
4 - 5	199.2	Compressive	
5 - 6	202.3	Compressive	206.9 ± 5.9
6 - 7	208.8	Tensile	
7 - 8	214.8	Tensile	
8 - 1	215.0	Tensile	

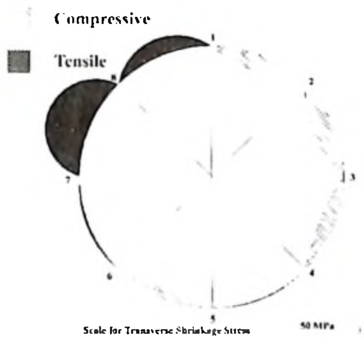

Fig. 8 : At a given heat input and ϕ of 8 kJ/cm and 0.25 respectively the distribution of transverse shrinkage stress at different quadrants of pipe weld preparedby using P-GMAW and conventional V-Groove.

Weld location	Transverse Shrinkage Stress (MPa)	Nature	Avg. Transverse Shrinkage Stress ± Std.Dev.
1 - 2	202.0	Compressive	
2 - 3	200.6	Compressive	
3 - 4	203.3	Compressive	
4 - 5	213.1	Tensile	
5 - 6	207.4	Compressive	212.6 ± 12.6
6 - 7	214.1	Tensile	
7 - 8	237.7	Tensile	
8 - 1	222.7	Tensile	

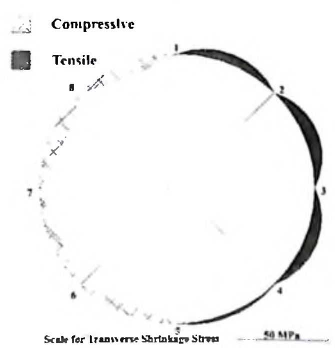

Fig. 9 : At a given heat input and ϕ of 9.1 kJ/cm and 0.06 respectively the distribution of transverse shrinkage stress at different quadrants of pipe weld preparedby using P-GMAW and conventional V-Groove.

Weld location	Transverse Shrinkage Stress (MPa)	Nature	Avg. Transverse Shrinkage Stress ± Std.Dev.
1 - 2	228.5	Tensile	
2 - 3	229.5	Tensile	
3 - 4	227.5	Tensile	
4 - 5	224.2	Tensile	
5 - 6	217.0	Compressive	221.8 ± 6.3
6 - 7	217.8	Compressive	
7 - 8	214.3	Compressive	
8 - 1	215.8	Compressive	

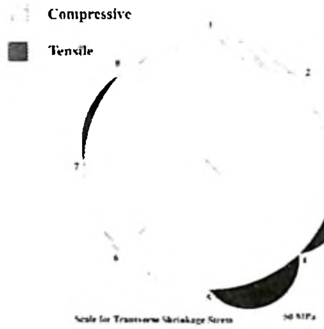

Fig. 10 : At a given heat input and ф of 9.4 kJ/cm and 0.25 respectively the distribution of transverse shrinkage stress at different quadrants of pipe weld preparedby using P-GMAW and conventional V-Groove.

Weld location	Transverse Shrinkage Stress (MPa)	Nature	Avg. Transverse Shrinkage Stress ± Std.Dev.
1 - 2	224.4	Compressive	235.9 ± 9.2
2 - 3	230.5	Compressive	
3 - 4	245.7	Tensile	
4 - 5	252.0	Tensile	
5 - 6	234.0	Compressive	
6 - 7	229.9	Compressive	
7 - 8	239.7	Tensile	
8 - 1	231.4	Compressive	

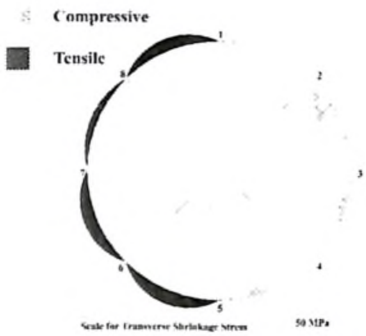

Fig. 11 : At a given heat input and ф of 7.4 kJ/cm and 0.05 respectively the distribution of transverse shrinkage stress at different quadrants of pipe weld preparedby using P-GMAW and conventional V-Groove.

Weld location	Transverse Shrinkage Stress (MPa)	Nature	Avg. Transverse Shrinkage Stress ± Std.Dev.
1 - 2	158.6	Compressive	166.1 ± 8.1
2 - 3	154.3	Compressive	
3 - 4	161.9	Compressive	
4 - 5	161.3	Compressive	
5 - 6	174.0	Tensile	
6 - 7	176.2	Tensile	
7 - 8	169.9	Tensile	
8 - 1	172.7	Tensile	

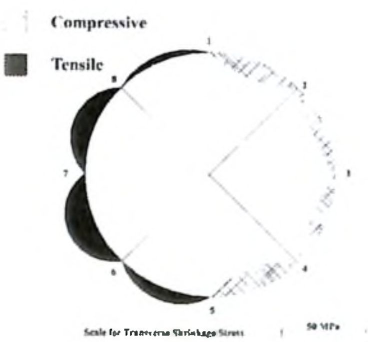

Fig. 12 : At a given heat input and ф of 8 kJ/cm and 0.25 respectively the distribution of transverse shrinkage stress at different quadrants of pipe weld preparedby using P-GMAW and conventional V-Groove.

Weld location	Transverse Shrinkage Stress (MPa)	Nature	Avg. Transverse Shrinkage Stress ± Std.Dev.
1 - 2	157.6	Compressive	169.1 ± 12.0
2 - 3	160.9	Compressive	
3 - 4	160.0	Compressive	
4 - 5	155.9	Compressive	
5 - 6	176.6	Tensile	
6 - 7	186.3	Tensile	
7 - 8	182.4	Tensile	
8 - 1	173.4	Tensile	

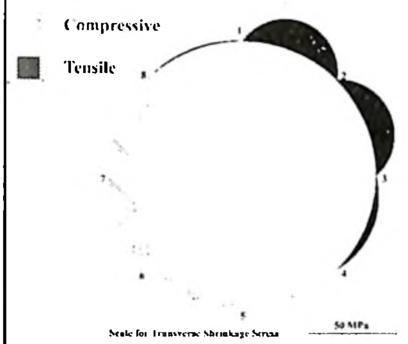

Fig. 13 : At a given heat input and ϕ of 9.2 kJ/cm and 0.06 respectively the distribution of transverse shrinkage stress at different quadrants of pipe weld preparedby using P-GMAW and conventional V-Groove.

Weld location	Transverse Shrinkage Stress (MPa)	Nature	Avg. Transverse Shrinkage Stress ± Std.Dev.
1 - 2	211.9	Tensile	195.3 ± 11.6
2 - 3	210.2	Tensile	
3 - 4	198.8	Tensile	
4 - 5	193.6	Compressive	
5 - 6	189.5	Compressive	
6 - 7	181.4	Compressive	
7 - 8	180.9	Compressive	
8 - 1	195.9	Tensile	

Table : 1
Reported values of measured transverse shrinkage at various locations of stainless steel pipe weld under different welding conditions (7, 12).

Process	Type of weld groove	No. of weld layers (N)	Heat input (Ω), (kJ/cm)	ϕ	Measured transverse shrinkage at various locations of steinless steel pipe weld, (mm)							
					1-1	**2-2**	**3-3**	**4-4**	**5-5**	**6-6**	**7-7**	**8-8**
GMAW	V-Groove	8	10.7	--	6.58	6.56	5.70	6.26	6.64	6.88	5.98	5.95
P - GMAW	V - Groove		7.7	0.05	5.64	6.06	5.69	5.96	5.52	5.59	5.56	5.41
			8.0	0.25	5.60	5.89	5.91	6.61	6.23	5.75	6.02	6.25
			9.1	0.06	5.45	5.23	5.25	5.09	5.11	5.25	5.44	5.56
			9.4	0.25	5.25	5.09	5.18	5.23	5.68	4.94	6.02	6.15
	NG - 13		7.4	0.05	5.39	5.46	5.30	4.88	5.03	4.67	4.62	4.64
			8.0	0.25	4.34	3.78	4.12	4.17	4.09	4.82	4.20	4.50
			9.2	0.06	4.08	3.99	4.25	3.94	4.04	5.00	4.54	4.80

Table 2 :
Estimation of the $\sigma_{tr(i-i)}$, and $\sigma_{(i-j)}$ is typically shown for the V-groove pipe weld prepared by MMAW process

Estimation of the $\sigma_{tr(i-i)}$	Estimation of the $\sigma_{tr(i-j)}$
$\sigma_{tr}(1\text{-}1) = \frac{6.58}{8} \times \frac{3.13}{25} \times \frac{2\times10^5}{80} = 257.03$ MPa	$\sigma_{tr}(1\text{-}2) = \frac{\sigma_{tr(1-1)} + \sigma_{tr(2-2)}}{2} = \frac{257.03 + 256.25}{2} = 256.64$ MPa
$\sigma_{tr}(2\text{-}2) = \frac{6.56}{8} \times \frac{3.2}{25} \times \frac{2\times10^5}{80} = 256.25$ MPa	$\sigma_{tr}(2\text{-}3) = \frac{\sigma_{tr(2-2)} + \sigma_{tr(3-3)}}{2} = \frac{256.25 + 242.25}{2} = 249.25$ MPa
$\sigma_{tr}(3\text{-}3) = \frac{5.70}{8} \times \frac{3.4}{25} \times \frac{2\times10^5}{80} = 242.25$ MPa	$\sigma_{tr}(3\text{-}4) = \frac{\sigma_{tr(3-3)} + \sigma_{tr(4-4)}}{2} = \frac{242.25 + 261.35}{2} = 251.80$ MPa
$\sigma_{tr}(4\text{-}4) = \frac{6.26}{8} \times \frac{3.34}{25} \times \frac{2\times10^5}{80} = 261.35$ MPa	$\sigma_{tr}(4\text{-}5) = \frac{\sigma_{tr(4-4)} + \sigma_{tr(5-5)}}{2} = \frac{261.35 + 273.90}{2} = 267.60$ MPa
$\sigma_{tr}(5\text{-}5) = \frac{6.64}{8} \times \frac{3.3}{25} \times \frac{2\times10^5}{80} = 273.90$ MPa	$\sigma_{tr}(5\text{-}6) = \frac{\sigma_{tr(5-5)} + \sigma_{tr(6-6)}}{2} = \frac{273.90 + 279.50}{2} = 276.70$ MPa
$\sigma_{tr}(6\text{-}6) = \frac{6.88}{8} \times \frac{3.25}{25} \times \frac{2\times10^5}{80} = 279.5$ MPa	$\sigma_{tr}(6\text{-}7) = \frac{\sigma_{tr(6-6)} + \sigma_{tr(7-7)}}{2} = \frac{279.50 + 231.72}{2} = 255.61$ MPa
$\sigma_{tr}(7\text{-}7) = \frac{5.98}{8} \times \frac{3.2}{25} \times \frac{2\times10^5}{80} = 231.72$ MPa	$\sigma_{tr}(7\text{-}8) = \frac{\sigma_{tr(7-7)} + \sigma_{tr(8-8)}}{2} = \frac{231.72 + 238.00}{2} = 234.86$ MPa
$\sigma_{tr}(8\text{-}8) = \frac{5.95}{8} \times \frac{3.2}{25} \times \frac{2\times10^5}{80} = 238.00$ MPa	$\sigma_{tr}(8\text{-}1) = \frac{\sigma_{tr(8-8)} + \sigma_{tr(1-1)}}{2} = \frac{238.00 + 257.03}{2} = 247.51$ MPa
Estimation of the σ_{avg}	$\sigma_{avg} = \frac{257.03 - 256.25 + 242.25 + 261.35 + 273.9 + 279.5 + 231.72 + 238.0}{8} = 255.00$ MPa
Estimation of the S.D	$\text{S.D.} = \sqrt{\left[\frac{1}{8} \times \begin{matrix} (257.03 - 255)^2 + (256.25 - 255)^2 + (242.25 - 255)^2 + (261.35 - 255)^2 + 273.9 - 255)^2 \\ (279.5 - 255)^2 + (231.72 - 255)^2 + (238-255)^2 \end{matrix}\right]}$ $= \pm\ 16.05$ MPa

Table : 3
At various locations of stainless steel pipe weld the estimated transverse shrinkage stress under different welding conditions

Process	Type of weld groove	Heat input (Ω), (kJ/cm)	ф	Estimated transverse shrinkage stress at various locatins of stainless steel pipe weld, (MPa)								
				1-1	**2-2**	**3-3**	**4-4**	**5-5**	**6-6**	**7-7**	**8-8**	Avg. ± Std. Groove
GMAW	V-Groove	10.7	--	257.03	256.25	242.25	261.35	273.90	279.50	31.72	238.00	255.00 ± 16.05
P - GMAW	V - Groove	7.7	0.05	212.89	204.30	205.08	198.83	199.61	205.08	212.50	217.19	206.94 ± 6.60
		8.0	0.25	205.08	198.83	202.34	204.30	221.88	192.97	235.16	240.23	212.60 ± 17.58
		9.1	0.06	220.31	236.72	222.27	232.81	215.63	218.36	217.19	211.33	221.83 ± 8.68
		9.4	0.25	218.75	230.08	230.86	260.55	243.36	224.61	235.16	244.14	235.94 ± 13.16
	NG - 13	7.4	0.05	169.53	147.66	160.94	162.89	159.77	188.28	164.06	175.78	166.11 ± 12.06
		8.0	0.25	159.38	155.86	166.02	153.91	157.81	195.31	177.34	187.50	169.14 ± 15.72
		9.2	0.06	210.55	213.28	207.03	190.63	196.48	182.42	180.47	181.25	195.26 ± 13.63

Table - 4 : X-ray radiography results of GMAW and P-GMAW joints

Process	Type of weld groove	Heat input (Ω), (kJ/cm)	ф	Proportion of defects discarded (%)	Location of defective quadrants	Type of defects
GMAW	V-Groove	10.7	--	17.1	2-6	Lack of fusion in groove wall
P-GMAW	V-Groove	7.7	0.05	10.1	2-5	Lack of fusion in groove wall
	NG-13	7.4	0.05	9.8	2-5	Lack of fusion in groove wall